MALAYSIAN JOURNAL OF SCIENCE
MJS
ISSN 1394-3065

Regular Issue

Malaysian Journal of Science 43(1): 44-58 (March 2024) https://mjs.um.edu.my

AN EFFECTIVE COMPUTATIONAL SCHEME FOR SOLVING VARIOUS MATHEMATICAL FRACTIONAL DIFFERENTIAL MODELS VIA NON-DYADIC HAAR WAVELETS

Ratesh Kumar[1a] and Jaya Gupta[2a]*

Abstract: The non-dyadic Haar wavelet (Haar scale-3) collocation approach is used in this article to generate numerical solutions for fractional differential equations. The non-linear fractional ordinary differential equations are linearised using the Quasilinearisation technique. The Haar scale-3 wavelet approach works by transforming a set of differential calculations into a set of linear algebraic equations. The reliability of the numerical solution can be improved by raising the degree of resolution, and error analysis can be performed. The numerical examples were solved to test the simplicity and flexibility of the method. The outcomes of the numerical examples are compatible with the exact solution and provide better results than previous results existing in the literature. This means that the procedure used here is consistent, reliable, and convenient to use.

Keywords: *Non-dyadic Haar wavelet (HS3WM), Quasilinearisation technique, fractional differential equation, non-linear ordinary differential equation, Riccati fractional equation*

1. Introduction

In recent years, the usage of fractional-order derivatives has exploded in engineering and biological sciences, as well as other fields of study. Modelling and controlling numerous dynamic systems is one of the biggest advantages of using fractional differential equations. Fractional derivatives and integrals are more useful and cost-effective than conventional derivatives in formulating specific electrochemical applications (Oldham & Spanier, 1974). This discovery stimulated their curiosity not only in the applications of the concepts of arbitrary order integrals and derivatives but also in the fundamental mathematical features of these interesting operators (Li & Zeng, 2015). Many physical phenomena, such as the behaviour of biological and mechatronic systems, rheology, complex viscoelasticity, anomalous diffusion, and so on, cannot be well defined and justified based on partial calculus. This has led researchers to explore alternative approaches, as highlighted by Baleanu and Shiri (2015), Miller and Ross (1993), and Podlubny (1993). In distinct fields such as science and engineering, fractional differential equations have many practical applications. Numerous substantial and technical structures, such as dielectric polarisation methods, viscoelastic systems, and electrode-electrolyte polarisation, are modelled using fractional derivatives (Almeida & Bastos, 2016; Gowrisankar & Uthayakumar, 2016). As a result of the expanding applications, many numerical approaches for solving these equations have been developed, including the wavelet method (Chen et al., 2012), the generalised differential transform method, the modified homotopy method (Odibat & Momani, 2008), the finite difference method (Sun et al., 2012), and so on. Non-linear phenomena can be seen in several scientific fields, including fluid dynamics, plasma physics, solid-state physics, chemical kinetics, engineering, and other fields. The mathematical technique of wavelet analysis is well-known and extensively applied. Wavelets are a set of expressions that have been combined to generate a sum of basic functions, and to generate these basic functions, a mother wavelet is translated and compressed. Therefore, it produces locality and smoothness properties. The use of wavelets has aroused researchers' interest in solving conventional ordinary and partial differential equations numerically. Numerous traditional wavelet techniques for solving these equations have recently been expanded by researchers. Numerical solutions and numerical integration of fractional ordinary and partial differential equations are two further wavelet applications in practical mathematics. For the time being, wavelets such as the B-spline, Legendre wavelet, Haar wavelet, Daubechies wavelet and Boubaker wavelet are used (Kobra & Mohsen, 2021). Many studies have employed the Haar scale wavelet, a wavelet that is orthonormal with compact support (Saeed & Rehman, 2013; Shah et al., 2017). A fractional differential equation is converted into an algebraic structure with a finite number of variables by using Haar wavelets (Amin et al., 2021). In 2018, HS3WM was used by Mittal and Pandit to solve a variety of differential equations and expressed that many various types of mathematical models controlled by differential equations, such as dispersive equations (Kumar & Gupta, 2022) and second-order linear integrodifferential equations (Kumar & Bakhtawar, 2022), can be equally capable of solving these wavelet bases (Mittal et al.,

Authors information:
[a]Department of Mathematics, Lovely Professional University, Punjab- 144411, INDIA. E-mail: rateshqadian@gmail.com.q[1]; jayagupta9295@gmail.com[2]
*Corresponding Author: jayagupta9295@gmail.com

Received: February 24, 2022
Accepted: September 18, 2023
Published: March 31, 2024

DOI:https//doi.org/10.22452/mjs.vol43no1.5
Malaysian Journal of Science 43(1): 44-58 (March 2024)

2018). They also depicted that, in terms of convergence, the HS3WM is more rapidly convergent than the Haar scale-2 wavelet. Furthermore, the attributes of the solution to the non-linear fractional differential equation are yet to be investigated using HS3WMs. This inspires us to introduce a new technique for analysing the behaviour of fractional equation-governed systems by employing the HS3WM.

The following types of differential equations are used to assess the applicability of modified HS3WM (Arora et al., 2020).

$$Du^{\alpha}(z) = G(z, u(z), u'(z), u"(z)) \quad (1)$$

With the given set of initial and boundary conditions,

Initial conditions: $u(0) = \mu_1$ and $u'(0) = \mu_2$ (2)

Dirichlet boundary conditions: $u(0) = \mu_3$ and $u(1) = \mu_4$ (3)

The manuscript is organised in the following sections: The fundamental definitions of fractional calculus are provided in Section 2. The HS3W and structure of its family in explicit forms, as well as the process for finding their integrals, were briefly discussed in Section 3. Section 4 explains the Quasilinearisation technique to solve a non-linear term in a differential equation. In Section 5, the present approach is used to solve five distinct models of fractional differential equations to evaluate their efficiency and performance. The conclusion drawn from the data, as well as future study ideas, is presented in Section 6.

2. Basic Definition of Fractional Calculus

In the given section, we discussed the basic definitions of fractional differentiation and integration.

Reimann Liouville Fractional differential operator of order α: For the positive real numbers α, t across the interval [m, n], the fractional differential operator established by Riemann-Liouville is given by Das (2011):

$$d^{\alpha}f(t) = \frac{1}{\Gamma(p-\alpha)}\left[\frac{d}{dt}\right]^{p}\int_{m}^{n} f(x)(t-x)^{p-\alpha-1}dx$$

where α denotes the order of the derivative and $t\epsilon$ [m, n].

Caputo fractional differential operator of order α: For positive real numbers α, t, the fractional differential operator developed by Caputo, an Italian mathematician, is (Shah et al., 2022):

$$d^{\alpha}f(t) = \frac{1}{\Gamma(p-\alpha)}\int_{m}^{n}\left[\frac{d}{dt}\right]^{p} f(x)(t-x)^{p}dx$$

where α denotes the order of the derivative and $t\epsilon$ [m, n].

3. Haar Scale-3 Wavelet

The main difference between Haar scale-2 wavelets is that the construction of the entire wavelet family can be done only by one mother wavelet, whereas in the HS3W, for the construction of the entire wavelet family, two distinct shapes of mother wavelets are responsible. Due to this, with the help of HS3W, the rate of convergence of the solution has increased. With dilation factor three, the family of HS3W with detailed information about Haar function, father wavelet, and symmetric and antisymmetric mother wavelets is provided below (Arora et al., 2020; Shiralashetti & Deshi, 2016).

$$f(z) \approx c_1\phi_1(z) + \sum_{even\ index\ i\geq 2}^{\infty} c_i\varphi_i^1(z) + \sum_{odd\ index\ i\geq 3}^{\infty} c_i\varphi_i^2(z)$$

Hence, the generalised form of the HS3-W family can be expressed in the form of:

$$h_i(t) = \phi(t) = \begin{cases} 1 & , \ a \leq t < b \\ 0 & , \ otherwise \end{cases} for\ i = 1$$

$$h_i(t) = \varphi_i^1(3^j - k) = \frac{1}{\sqrt{2}}\begin{cases} -1 & \chi_{11}(i) \leq t < \chi_{12}(i) \\ 2 & \chi_{12}(i) \leq t < \chi_{13}(i) \\ -1 & \chi_{13}(i) \leq t < \chi_{14}(i) \\ 0 & otherwise \end{cases} for\ i = 2,4,6\ldots\ldots,3p-1$$

DOI:https//doi.org/10.22452/mjs.vol43no1.5
Malaysian Journal of Science 43(1): 44-58 (March 2024)

$$h_i(t) = \varphi_i^2(3^j - k) = \sqrt{\frac{3}{2}} \begin{cases} 1 & \chi_{11}(i) \le t < \chi_{12}(i) \\ 0 & \chi_{12}(i) \le t < \chi_{13}(i) \\ -1 & \chi_{13}(i) \le t < \chi_{14}(i) \\ 0 & otherwise \end{cases} \quad for\ i = 1,3,5\ldots\ldots,3p$$

$\chi_{11}(i) = a + (b-a)\frac{k}{p}, \chi_{12}(i) = a + (b-a)\frac{3k+1}{3p}, \quad \chi_{13} = a + (b-a)\frac{3k+2}{3p}, \quad \chi_{14} = a + (b-a)\frac{k+1}{p}.$ Here, $p = 3^j, j = 0,1,2,3,\ldots\ldots, k = 0,1,2,\ldots\ldots, p-1.$

The translation characteristics, resolution level (dilation factor), and wavelet number of the wavelet family are represented by k, j, and i, respectively. We defined integrals for HS3W as follows:

$$\int_0^x \phi_{i,s}(r)dr = \phi_{i,s+1}(r) = \begin{cases} \frac{r^s}{\Gamma(s+1)} & , \quad a \le r < b \\ 0 & otherwise \end{cases}$$

$$\int_0^x \varphi_{i,s}{}^1(r)dr = \varphi_{i,s+1}{}^1(r) = \frac{1}{\sqrt{2}} \begin{cases} 0 & ; 0 \le r < \chi_{11}(i) \\ \frac{-[r-\chi_{11}(i)]^s}{\Gamma(s+1)} & ; \chi_{11}(i) \le r < \chi_{12}(i) \\ \frac{3[r-\chi_{12}(i)]^s - [r-\chi_{11}(i)]^s}{\Gamma(s+1)} & ; \chi_{12}(i) \le r < \chi_{13}(i) \\ \frac{3[r-\chi_{12}(i)]^s - 3[r-\chi_{13}(i)]^s - [r-\chi_{11}(i)]^s}{\Gamma(s+1)} & ; \chi_{13}(i) \le r < \chi_{14}(i) \\ \frac{3[r-\chi_{12}(i)]^s - 3[r-\chi_{13}(i)]^s - [r-\chi_{11}(i)]^s + [r-\chi_{14}(i)]^s}{\Gamma(s+1)} & ; \chi_{14}(i) \le r < 1 \end{cases}$$

$$\int_0^x \varphi_{i,s}{}^2(r)dr = \varphi_{i,s+1}{}^2(r) = \sqrt{\frac{3}{2}} \begin{cases} 0 & ; 0 \le r < \chi_{11}(i) \\ \frac{[r-\chi_{11}(i)]^s}{\Gamma(s+1)} & ; \chi_{11}(i) \le r < \chi_{12}(i) \\ \frac{[r-\chi_{11}(i)]^s - [r-\chi_{12}(i)]^s}{\Gamma(s+1)} & ; \chi_{12}(i) \le r < \chi_{13}(i) \\ \frac{[r-\chi_{11}(i)]^s - [r-\chi_{12}(i)]^s - [r-\chi_{13}(i)]^s}{\Gamma(s+1)} & ; \chi_{13}(i) \le r < \chi_{14}(i) \\ \frac{[r-\chi_{11}(i)]^s - 3[r-\chi_{12}(i)]^s - [r-\chi_{13}(i)]^s + [r-\chi_{14}(i)]^s}{\Gamma(s+1)} & ; \chi_{14}(i) \le r < 1 \end{cases}$$

4. Quasilinearisation Technique

Basically, the Quasilinearisation technique is a generalised form of the Newton-Raphson technique. It converges to a solution in its exact form. Quadratically, it must show monotone convergence (Saeed & Rehman, 2013). Here, consider a non-linear second-order differential equation:

$$\psi''(v) = k(v, \psi(v)) \qquad (4)$$

With boundary conditions:

$$\psi(a_1) = \theta_1, \psi(b_1) = \theta_2;\ a_1 \le v \le b_1$$

Here, k is in terms of $\psi(v)$. Let us choose an approximation at the initial step of solution $\psi(v)$. Let us say $\psi_0(v)$. k can be expanded around $\psi_0(v)$ and is written in the form

$$k(\psi(v), v) = k(\psi_0(v), v) + (\psi(v) - \psi_0(v))k_{\psi_0(v)}(\psi_0(v), v) \qquad (5)$$

$$\psi''(v) = k(\psi_0(v), v) + (\psi(v) - \psi_0(v))k_{\psi_0(v)}(\psi_0(v), v) \qquad (6)$$

$$\psi''(v) = k(\psi_1(v), v) + (\psi(v) - \psi_1(v))k_{\psi_1(v)}(\psi_1(v), v) \qquad (7)$$

The form of a recurrence relationship is:

$$\psi_{s+1}{}''(v) = k(\psi_s(v), v) + (\psi(v) - \psi_s(v))k_{\psi_s(v)}(\psi_s(v), v) \qquad (8)$$

for obtaining $\psi_{s+1}(v)$, here, use $\psi_s(v)$, whose value is already known. A non-linear differential equation with the required conditions is given as follows:

DOI:https//doi.org/10.22452/mjs.vol43no1.5
Malaysian Journal of Science 43(1): 44-58 (March 2024)

$$\psi_{s+1}(\upsilon) = \alpha, \psi_s(\upsilon) = \beta. \quad (9)$$

Now, consider the non-linear second-order differential equation of the form:

$$\psi''(\upsilon) = k(\psi'(\upsilon), \psi(\upsilon), \upsilon)$$

Here, the first derivative $q'(m)$ can be considered as another function

$$\psi_{s+1}{}''(\upsilon) = k(\psi'(\upsilon), \psi(\upsilon), \upsilon) + (\psi'_{s+1}(\upsilon) - \psi'_s(\upsilon))\, k_{\psi'_s(\upsilon)}(\psi'_s(\upsilon), \psi_s(\upsilon), \upsilon)) + (\psi_{s+1}(\upsilon) - \psi_s(\upsilon))\, \mathrm{k}\, (\psi'_s(\upsilon), \psi_s(\upsilon), \upsilon) \quad (10)$$

With boundary conditions $\psi_{s+1}(\upsilon) = \alpha, \psi_s(\upsilon) = \beta.$ (11)

Follow the same technique to establish the recurrence relation for higher-order non-linear differential equations.

$$L^j\psi_{s+1}(\upsilon) = k(\psi_s(\upsilon), \psi'_s(\upsilon).\ldots\ldots \psi_s^{j-1}(\upsilon), \upsilon) + \sum_{p=0}^{n-1}(\psi^p_{s+1}(\upsilon) - \psi^p_s(\upsilon))\, k_{\psi^p}(\psi'_s(\upsilon), \psi_s(\upsilon), \ldots., \psi_s^{j-1}(\upsilon), \upsilon) \quad (12)$$

The order of the differential equation is j; the above equation is linear, and it can be solved recursively, $\psi_s(\upsilon)$, if it has a known value and can be used to get the value of $\psi_{s+1}(\upsilon)$.

5. Applications of Fractional Differential Equations

In this part, the HS3WM is used to solve certain numerical problems for solving linear as well as non-linear fractional differential equations and compare the results with the results obtained by methods available in the literature to demonstrate the method's compatibility.

Numerical Experiment No. 1: Fractional Riccati Equation

$$D^\alpha y(x) = -y^2(x) + 1, for\ x \geq 0, 0 \leq \alpha \leq 1 \quad (13)$$

Subject to the initial condition y (0) = 0.

exact solution at $\alpha = 1$,

$$y(x) = \frac{e^{2x}-1}{e^{2x}+1} \quad (14)$$

Solution:

Applying the Quasilinearisation technique to the non-linear term of equation (13), we get

$$D^\alpha y_{s+1}(x) + 2\, y_s(x) y_{s+1}(x) = y_s^2 + 1, x \geq 0 \quad (15)$$

With the initial condition $y_{s+1}(0) = 0$, we applied HS3WM to equation (15), and we approximated the term containing the highest derivatives by Haar wavelet series as follows:

$$D^\alpha y_{s+1}(x) = \sum_{l=1}^{3M} c_l h_l(x) \quad (16)$$

On integrating the above equation (16), we obtained the lower derivatives, and by using the initial condition, we have,

$$y_{s+1}(x) = \sum_{l=1}^{3M} c_l P_{\alpha,l}(x) \quad (17)$$

Now, substituting equations (16) and (17) in equation (15), we get

$$\sum_{l=1}^{3M} c_l[h_l(x) + 2\, y_s(x) P_{\alpha,l}(x)] = y_s^2(x) + 1 \quad (18)$$

DOI:https//doi.org/10.22452/mjs.vol43no1.5
Malaysian Journal of Science 43(1): 44-58 (March 2024)

For α = 1, we assigned the differential order to equation (13) and at J = 2 resolution level. Tables 1 and 2 show the comparative study of the exact and approximate solutions as well as the values of errors, respectively, derived using the Haar scale-3 wavelet technique, and graphical results are shown in Figure 1. The absolute inaccuracy decreases as the number of iterations increases. Using the Quasilinearisation technique at a given level of resolution, the precise answer at α = 1 and the Haar wavelet resolution at various $\alpha's$ are demonstrated in Figure 2.

Table 1. Comparison of Exact Value and Approximate Value at Different Values of *x* and Result Comparison by Two Different Methods

x	Exact Value	Approx. value	Absolute Error by HS3WM	Kobra, 2021
0.1	0.01851640192288	0.018512172212923	2.8650e-05	6.11e-05
0.2	0.05549847010902	0.055485850362306	4.2584e-05	1.16e-04
0.3	0.092328886151755	0.092308082564065	5.9053e-05	1.12e-04
0.4	0.128908385222714	0.128879735027882	6.7831e-05	8.34e-04
0.5	0.165140412924629	0.165104375053012	6.9465e-05	6.69e-03
0.6	0.200932122324545	0.200889264899714	6.6312e-05	6.64e-03
0.7	0.236195287939167	0.236146273143560	5.7972e-05	6.24e-04
0.8	0.270847118516721	0.270792685450088	4.6444e-05	5.86e-03
0.9	0.304810954186844	0.304751900397517	3.7996e-05	1.48e-04

Table 2. Comparison of Value of Error of L_2 Error and L_∞ Errors at Different Levels of Resolution.

Level of resolution	J=2	J=3	J=4	J=5
HSWM3 $L_2 error$	1.0785e-04	1.1896e-05	1.3217e-06	1.5412e-07
HSWM3 $L_\infty error$	6.9465e-05	7.7184e-06	8.5760e-07	9.7023e-08

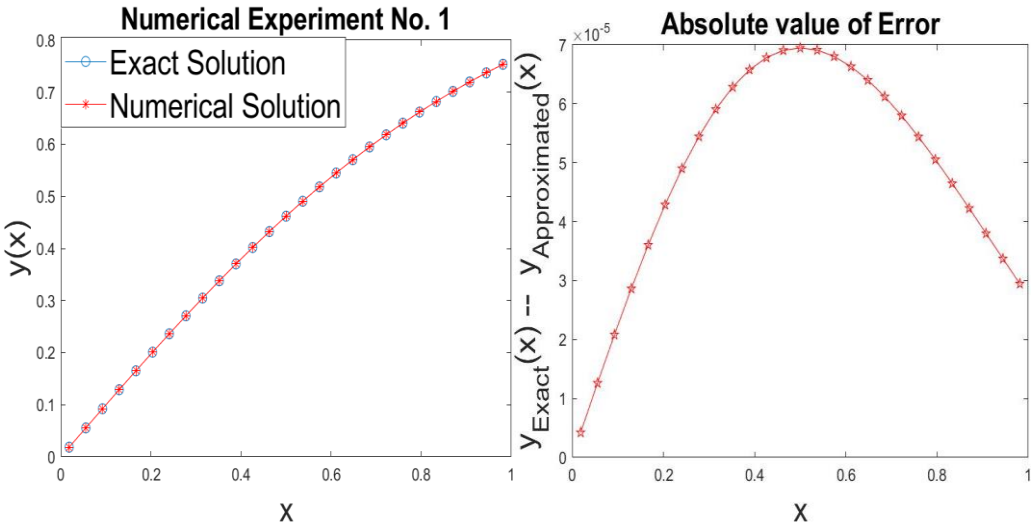

Figure 1. Graphical Representation of the Exact Solution and the Numerical Solution at $\alpha = 1$

DOI:https//doi.org/10.22452/mjs.vol43no1.5
Malaysian Journal of Science 43(1): 44-58 (March 2024)

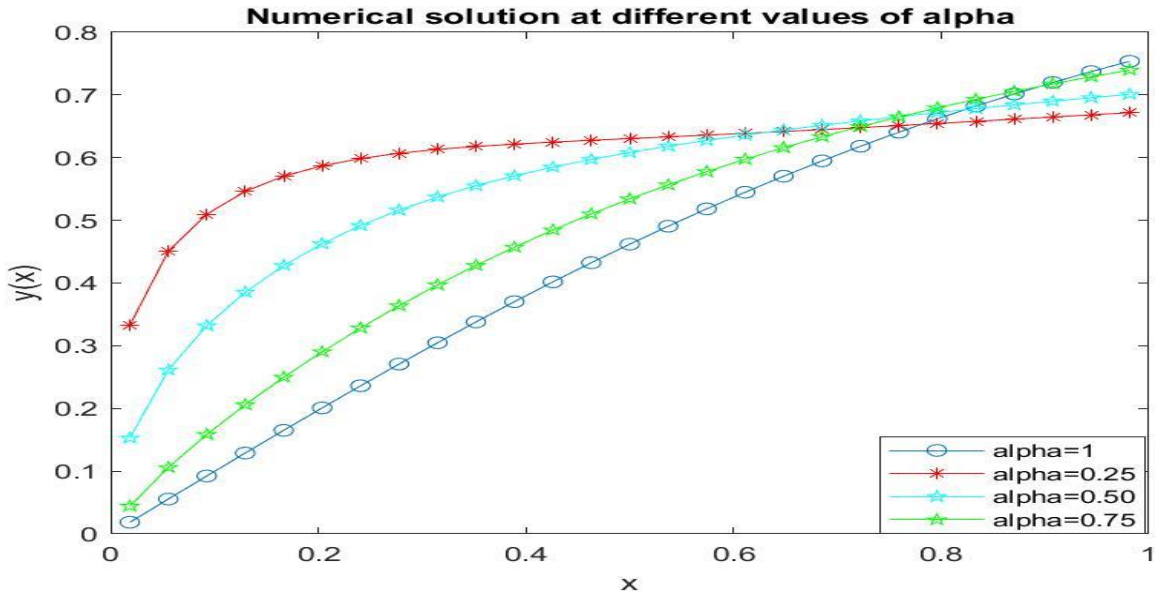

Figure 2. Graphical Representation of the Numerical Solution for Different Values of α Lies Between 0 and 1. At j = 2 Resolution Level.

Numerical Experiment No. 2: Fractional Vander-Pol Oscillator Problem

$$D^{\alpha}y(x) + \frac{dy(x)}{dx} + y(x) + y^2(x)\frac{dy(x)}{dx} = 2\,cos(x) - cos^3(x), \qquad 1 \le \alpha \le 2 \qquad (19)$$

Subject to early circumstances: y (0) = 0, $y'(0) = 1$
At $\alpha = 2$, the precise answer that exists in the literature (Odibat & Momani, 2008) is given by: y(x)= sin(x)
Solution: After applying the Quasilinearisation technique to equation (19), we get

$$D^{\alpha}y_{s+1}(x) + \big(1 + 2y_s(x){y_s}'(x)\big)y_{s+1}(x) + \big(1 + {y_s}^2(x)\big){y_{s+1}}'(x) = 2{y_s}'(x){y_s}^2(x) + 2cos(x) - cos^3(x), 1 \le \alpha \le 2 \qquad (20)$$

With the initial condition $y_{s+1}(0) = 0, {y_s}'(0) = 1$, we applied the Haar scale-3 method to (20), and we approximated the term with the highest derivatives by the Haar wavelet series as follows:

$$D^{\alpha}y_{s+1}(x) = \sum_{l=1}^{3M} c_l h_l(x) \qquad (21)$$

On integrating the above equation (21), we obtained the lower derivatives, and by using the initial condition, we have

$$y_{s+1}(x) = \sum_{l=1}^{3M} c_l P_{\alpha,l}(x) \qquad (22)$$

Now, substituting equations (21) and (22) in equation (20), we get

$$\sum_{l=1}^{3M} c_l[\,h_l(x) + (1 + 2y_s(x)\,{y_s}'(x))\,P_{\alpha,l}(x) + (1 + {y_s}^2(x))P_{\alpha-1,l}(x)] = 2{y_s}^2(x){y_s}'(x) - (1 + 2{y_s}'(x)y_s(x)\,)x - 1 - {y_s}^2(x) + 2cos(x) - cos^3(x) \qquad (23)$$

With initial approximations $y_0(x) = 0, {y_0}'(x) = 1$

We assigned the differential order to equation (20) for α = 2 and the level of resolution to J = 2. Tables 3 and 4 show the comparative study of the exact and approximate solutions as well as the values of errors, respectively, derived using the Haar scale-3 wavelet technique, and graphical results are shown in Figure 3. With more iterations, the absolute error decreases. The precise solution at α = 1 and the Haar wavelet solution at distinct $\alpha's$ are represented in Figure. 4 via the Quasilinearisation technique at a fixed level of resolution.

DOI:https//doi.org/10.22452/mjs.vol43no1.5
Malaysian Journal of Science 43(1): 44-58 (March 2024)

Table 3. Comparison of the Exact Value and the Approximate Value at Different Values of *x* and Discussion of Absolute Error by Scale-3 Haar Wavelets with Haar Scale Wavelets

x	Exact Value	Approx. value	Saeed, 2017	Absolute Error by HS3WM
0.1	0.0998334166	0.0998334056	0.0998333872	2.89934e-06
0.2	0.1986693308	0.1986693108	0.1986692768	8.67113e-06
0.3	0.2955202067	0.2955202012	0.2955201331	1.44070e-05
0.4	0.3894183423	0.3894182990	0.3894182543	2.01071e-05
0.5	0.4794255386	0.4794255100	0.4794254413	2.57714e-05
0.6	0.5646424734	0.5646423900	0.5646423719	3.13998e-05
0.7	0.6442176872	0.6442176329	0.6442175863	3.69924e-05
0.8	0.7173560909	0.7173560600	0.7173559950	4.25492e-05
0.9	0.7833269096	0.7833268874	0.7833268225	4.80701e-05

Table 4. Comparison of the Value of the Error of the Scale-3 Haar Wavelet at Different Levels of Resolution.

Level of resolution	J=2	J=3	J=4
HSWM3 $L_2 error$	6.33395260e-05	7.03695009e-06	7.81873793e-07
HSWM3 $L_\infty error$	4.12718973e-05	4.58592395e-06	5.09566047e-07

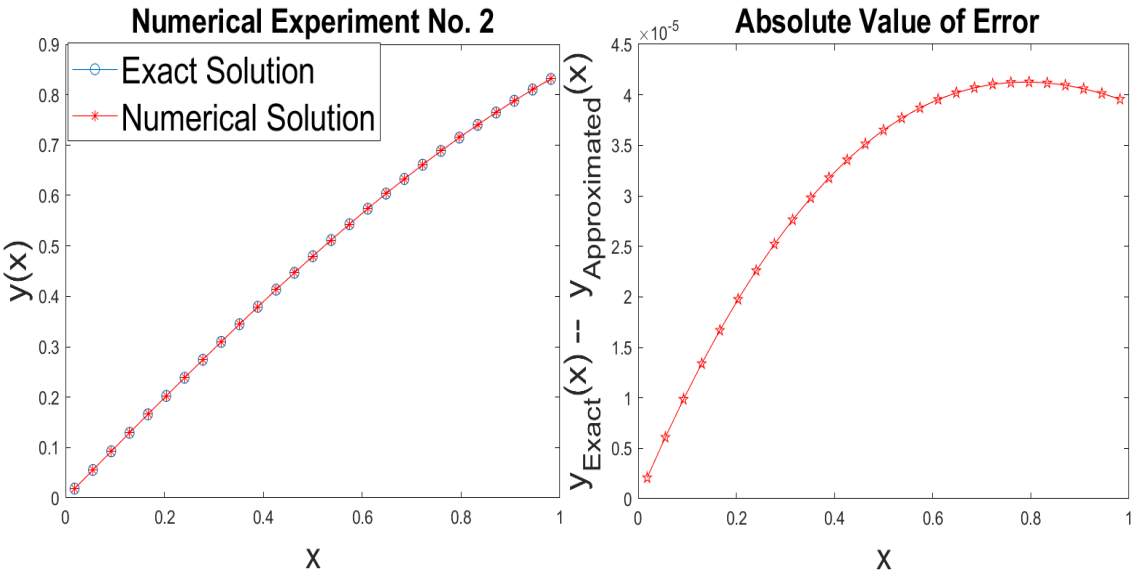

Figure 3. Graphical Representation of the Exact Solution and the Numerical Solution

DOI:https//doi.org/10.22452/mjs.vol43no1.5
Malaysian Journal of Science 43(1): 44-58 (March 2024)

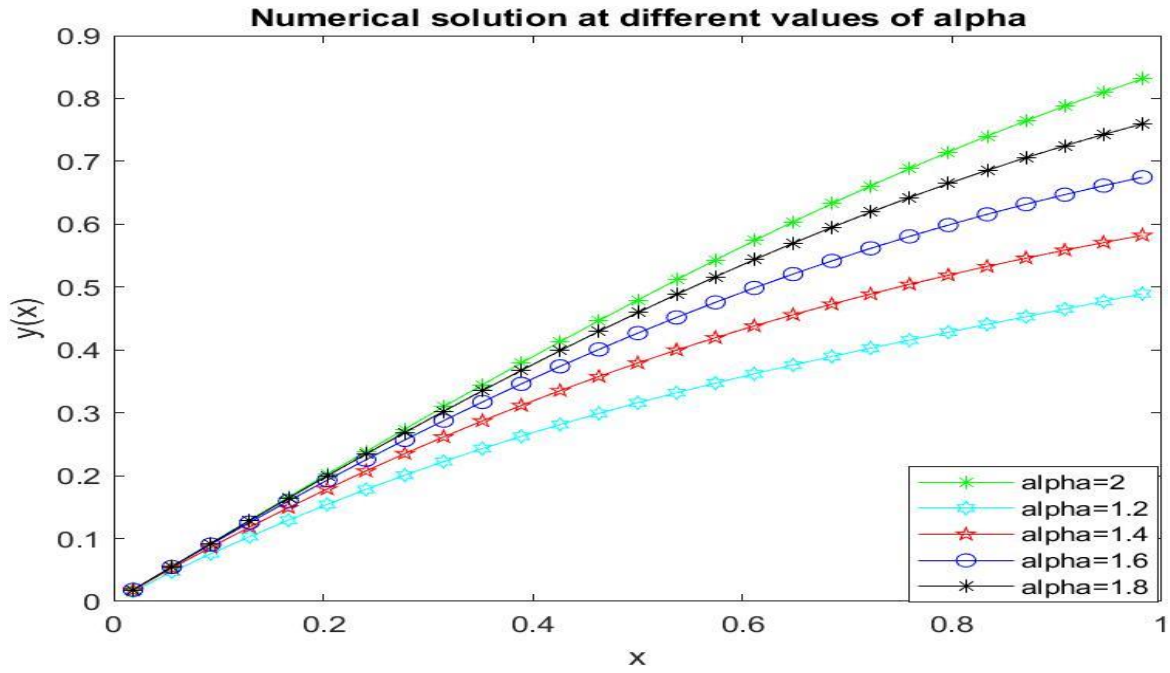

Figure 4. Graphical Representation of Numerical Solution for Different Values of α Lies Between 1 and 2. At *j = 2* Resolution Level

Numerical Experiment No. 3: Non-linear Oscillator Ordinary Differential Equation

$$D^{\alpha}y(x) + (y')^2(x) - y(x) + y^2(x) - 1 = 0, \quad 1 < \alpha \leq 2 \qquad (24)$$

With the initial condition y (0) = 2, $y'(0) = 0$
The value of the exact solution at $\alpha = 2$ given as,

y(x)=1+cos(x)

Solution:
Applying the Quasilinearisation technique to equation (24) and the equation becomes
$D^{\alpha}y_{s+1}(x) + 2y_s'(x)y_{s+1}'(x) - (1 - 2y_s(x))y_{s+1}(x) = y_s^2(x) + (y'_s)^2(x) + 1$ (25)
With the initial conditions $y_{s+1}(0) = 0, y_s'(0) = 0,$

We applied HS3WM to (24), and we approximated the term that contains the highest derivatives by Haar wavelet series as follows:

$$D^{\alpha}y_{s+1}(x) = \sum_{l=1}^{3M} c_l h_l(x) \qquad (26)$$

On integrating the above equation (26), we obtained the lower derivatives, and by using the initial condition, we have

$$y_{s+1}(x) = \sum_{l=1}^{3M} c_l P_{\alpha,l}(x) + 2 \qquad (27)$$

$$y'_{s+1}(x) = \sum_{l=1}^{3M} c_l P_{\alpha-1,l}(x) \qquad (28)$$

Now, substituting equations (26), (27), and (25) in equation (24), we get

$\sum_{l=1}^{3M} c_l[h_l(x) + 2y_s'(x)\, P_{\alpha-1,l}(x) - (1 - 2y_s'(x))\, P_{\alpha,l}(x)] =$ $y_s^2(x) + y_s'^2(x) + 2(1 - 2y_s(x)) + 1$ (29)

With initial conditions $y_0(x) = 0, y_0'(x) = 0$

DOI:https//doi.org/10.22452/mjs.vol43no1.5
Malaysian Journal of Science 43(1): 44-58 (March 2024)

For α = 2, we assigned the differential order to equation 25 and at J = 2 resolution level. Tables 5 and 6 show the comparative study of the exact and approximate solutions as well as the values of errors, respectively, derived using the Haar scale-3 wavelet technique, and graphical results are shown in Figure 5. The absolute inaccuracy decreases as the number of iterations increases. At a constant level of resolution, the exact solution at α = 1 and the Haar wavelet solutions at various $\alpha's$ are shown in Figure 6.

Table 5. Comparison of Exact Value and Approximate Value at Different Values of *x*. Discussion of Absolute Error by Scale-3 Haar Wavelets with Haar Scale Wavelets.

x	Exact Value	Approx Value	Saeed 2013	Absolute Error by HS3WM
0.1	1.995004165	1.995004166	1.995004166	3.734e-06
0.2	1.980066578	1.980066579	1.980066581	1.568e-05
0.3	1.955336489	1.955336492	1.955336496	3.958e-05
0.4	1.921060994	1.921060999	1.921061007	7.543e-05
0.5	1.877582562	1.877582576	1.877582583	1.232e-04
0.6	1.825335615	1.825335628	1.825335647	1.830e-04
0.7	1.764842187	1.764842204	1.764842233	2.547e-04
0.8	1.696706709	1.696706740	1.696706772	3.384e-04
0.9	1.621609968	1.621609998	1.621601051	4.341e-04

Table 6. Comparison of Values of the Error Scale-3 Haar Wavelet at Different Levels of Resolution.

Level of resolution	J=2	J=3	J=4
HSWM3 $L_2 error$	8.69048147e-06	9.66118381e-07	1.07352784e-07
HSWM3 $L_\infty error$	3.71196461e-05	4.25861607e-06	4.78242174e-07

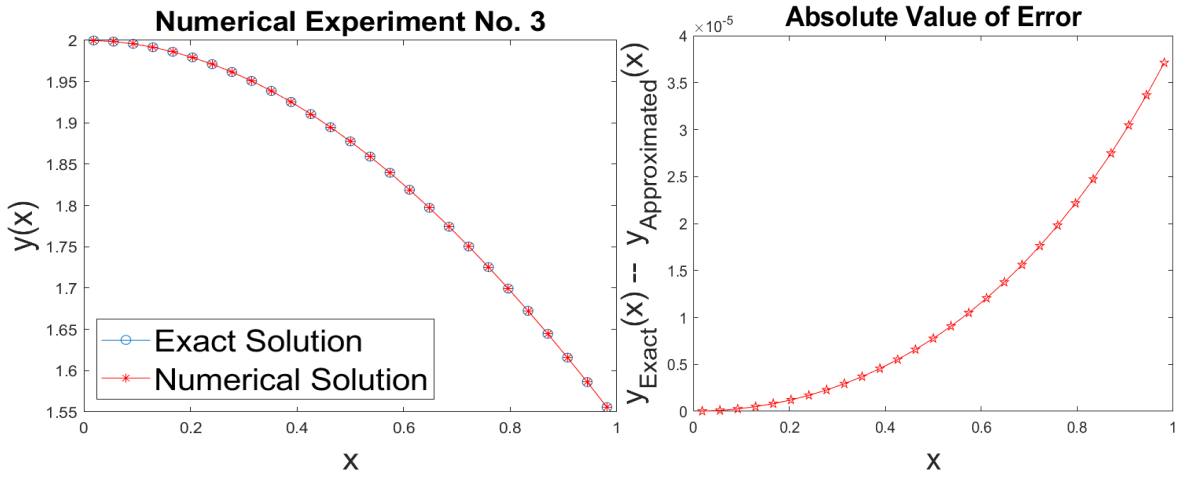

Figure 5. Graphical Representation of the Exact Solution and the Numerical Solution

DOI:https//doi.org/10.22452/mjs.vol43no1.5
Malaysian Journal of Science 43(1): 44-58 (March 2024)

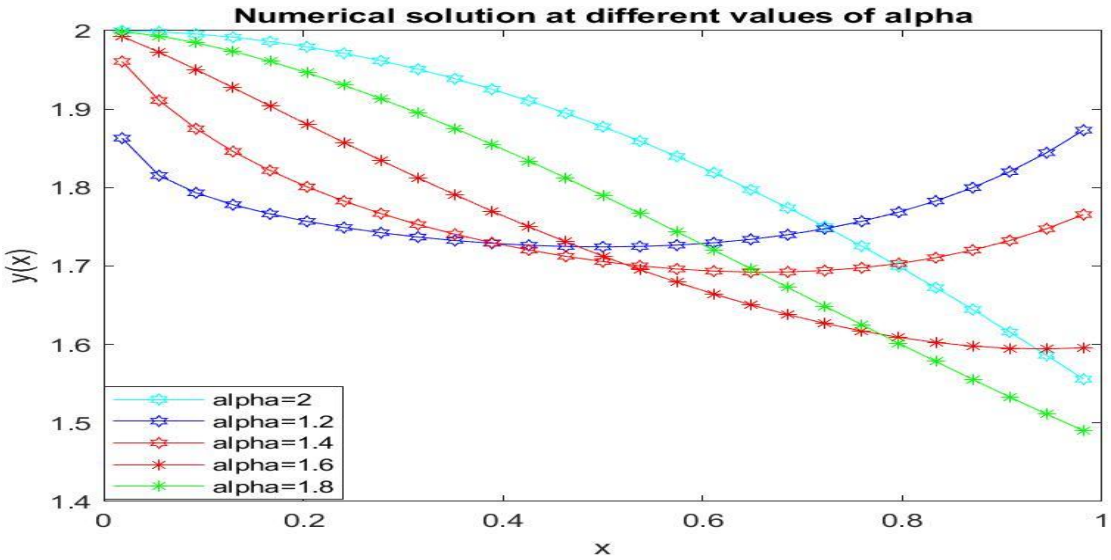

Figure 6. Graphical Representation of the Numerical Solution for Different Values of α Lies Between 1 and 2. At j = 2 Resolution Level.

Numerical Experiment No. 4: Composite Fractional Oscillation Equation

$$D^{\alpha}y(x) + y(x) = f(x), 0 < \alpha < 1 \qquad (30)$$

With initial condition $y(0) = 0$, where $f(x) = x^2 + \frac{2x^{2-\alpha}}{\Gamma(3-\alpha)}$ (31)

For $\alpha = 1$, the exact solution of the equation is y(x)=x^2

Solution:

We applied the Haar scale-3 method to (30), and we estimated the advanced derivatives term by Haar wavelet series as follows:

$$D^{\alpha}y(x) = \sum_{l=1}^{3M} c_l h_l(x) \qquad (32)$$

On integrating the above equation (32), we obtained the lower derivatives, and by using the initial condition, we have

$$y(x) = \sum_{l=1}^{3M} c_l P_{\alpha,l}(x) \qquad (33)$$

now using equations (33) and (32) in equation (30).

$$\sum_{l=1}^{3M} c_l[h_l(x) + P_{\alpha,l}(x)] = x^2 + \frac{2x^{2-\alpha}}{\Gamma(3-\alpha)} \qquad (34)$$

We assigned the differential order to equation 30 for α = 1 and the level of resolution to J = 2. Table 7 depicts the absolute error at α = 1 and other fractional values of alpha, and Table 8 presents the value of L_2 and L_∞ error at different values of J. Here, Figure 7 depicts the exact and approximate solutions obtained using the HS3WM approach. With more iterations, the absolute error decreases. The precise solution at α = 1 and the Haar wavelet solution at distinct $\alpha's$ are represented in Figure 8.

DOI:https//doi.org/10.22452/mjs.vol43no1.5
Malaysian Journal of Science 43(1): 44-58 (March 2024)

Table 7. Comparison of Exact Value and Approximate Value at Different Values of *x*. Discussion of Absolute Error by Scale-3 Haar Wavelet with Haar Scale Wavelets at Different Values of α

x	Exact Value $\alpha = 1$	Approx. Value $\alpha = 1$	Absolute error at $\alpha = 1$	Absolute Error by HS3WM $(\alpha = 0.25)$	Shah 2017	$(\alpha = 0.50)$	Shah 2017
0.1	0.01	0.0101	3.012e-04	4.225e-06	9.000e-03	4.1904e-06	4.000e-03
0.2	0.04	0.0414	2.797e-04	4.105e-06	8.000e-03	4.3903e-06	5.000e-03
0.3	0.09	0.0914	2.503e-04	4.004e-06	4.000e-03	4.0882e-06	1.000e-03
0.4	0.16	0.1609	2.224e-04	3.939e-06	2.800e-03	3.9885e-06	8.000e-03
0.5	0.25	0.2500	2.085e-04	3.875e-06	6.300e-03	3.9234e-06	2.300e-03
0.6	0.36	0.3634	1.816e-04	3.843e-06	3.200e-03	3.8435e-06	6.000e-03
0.7	0.49	0.4923	1.665e-04	3.812e-06	2.000e-03	1.6807e-06	7.000e-03
0.8	0.64	0.6406	1.490e-04	4.088e-06	9.000e-03	1.5997e-06	0.000
0.9	0.81	0.8159	1.384e-04	3.796e-06	5.200e-03	1.7160e-06	1.400e-03

Table 8. Comparison of the Value of Error of HS3WM at Different Levels of Resolution

Level of resolution	J=2	J=3	J=4
HS3WM $L_2 error$	5.0450146e-04	5.602634e-05	6.2247865e-06
HS3WM $L_\infty error$	3.3670033e-04	3.787018e-05	4.2250783e-06

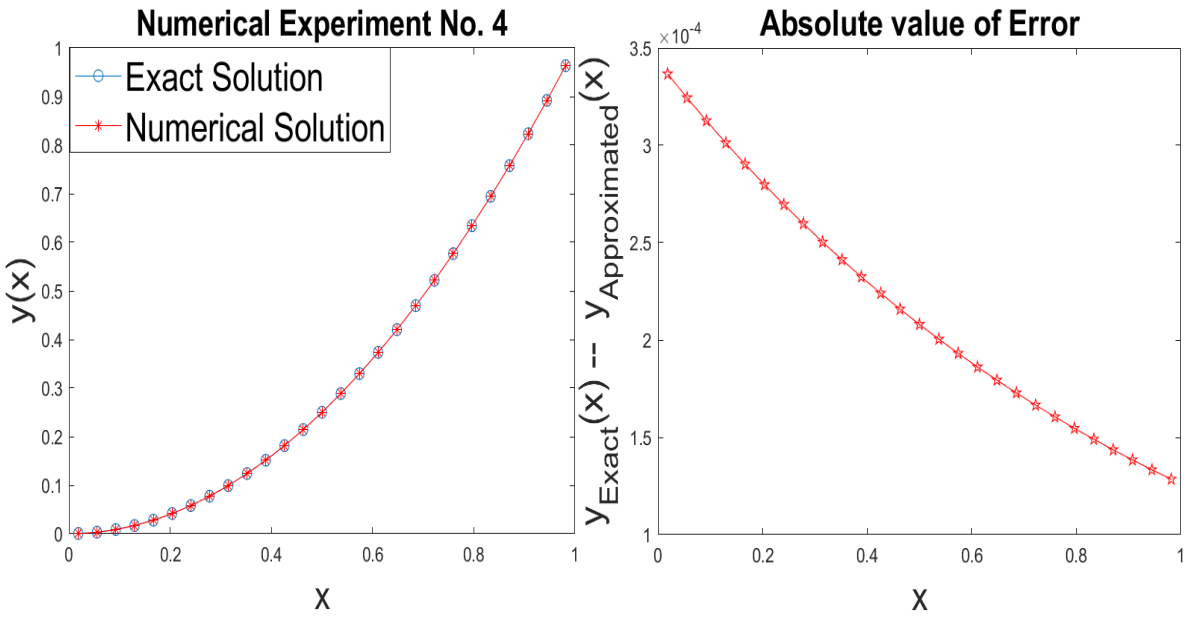

Figure 7. Graphical Representation of Exact Solutions and Numerical Solutions

DOI:https//doi.org/10.22452/mjs.vol43no1.5
Malaysian Journal of Science 43(1): 44-58 (March 2024)

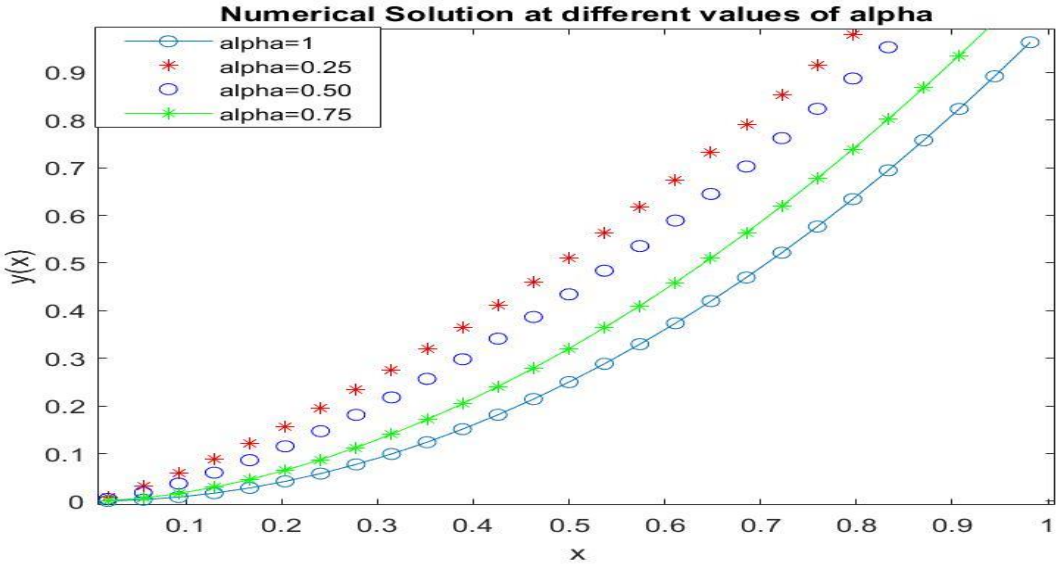

Figure 8. Graphical Representation of Numerical Solution for Different Values of α Lies Between 0 and 1. At *j = 2* Resolution Level.

Numerical Experiment No. 5: Fractional Relaxation-Oscillation Equation

$$\boldsymbol{D^{\alpha}y(x) + y(x) = f(x), 0 < \alpha < 1} \qquad (35)$$

With initial conditions y (0) = 0.

Here,

$$f(x)=1-4x+5x^2-\frac{4}{\Gamma(2-\alpha)}x^{1-2\alpha}+\frac{10}{\Gamma(3-\alpha)}x^{2-\alpha} \qquad (36)$$

for $\alpha = 1$, the exact solution of the given equation is $y(x) = 1-4x+5x^2$

Solution:
We applied HS3WM to (35) and approximated the term that has derivatives by Haar wavelet series as follows:

$$D^{\alpha}y(x) = \sum_{l=1}^{3M} c_l h_l(x) \qquad (37)$$

On integrating the above equation (37), we obtained the lower derivatives, and by using the initial condition, we have

$$y(x) = \sum_{l=1}^{3M} c_l P_{\alpha,l}(x) \qquad (38)$$

now using equations (37) and (38) in equation (35).

$$\sum_{l=1}^{3M} c_l[h_l(x) + P_{\alpha,l}(x)] = 1 - 4x + 5x^2 - \frac{4}{\Gamma(2-\alpha)}x^{1-2\alpha} + \frac{10}{\Gamma(3-\alpha)}x^{2-\alpha}$$

We assigned the differential order to equation 35 for α = 1 and the level of resolution to J = 2. Table 9 depicts the absolute error at α = 1 and other fractional values of alpha, and Table 10 presents the value of L_2 and L_∞ error at different values of J. Here, Figure 7 depicts the exact and approximate solutions obtained using the HS3WM approach. With more iterations, the absolute error decreases. The precise solution at α = 1 and the Haar wavelet solution at distinct $\alpha's$ are represented in Figure 8.

DOI:https//doi.org/10.22452/mjs.vol43no1.5
Malaysian Journal of Science 43(1): 44-58 (March 2024)

Table 9. Comparison of Exact Value and Approximate Value at Different Values of *x*. Discussion of Absolute Error by Scale-3 Haar Wavelet with Haar Scale Wavelets at Different Values of α.

x	Exact Value $\alpha = 1$	Approximate Value $\alpha = 1$	Absolute error at $\alpha = 1$	Absolute Error by HS3WM. $(\alpha = 0.25)$	Shah 2017	Absolute Error by HS3WM $(\alpha = 0.50)$	Shah 2017
0.1	0.6500	0.6475	1.506e-03	2.1038e-05	8.000e-03	2.0525e-05	2.300e-03
0.2	0.4000	0.4058	1.399e-03	2.0441e-05	1.700e-03	1.4646e-05	3.000e-03
0.3	0.2500	0.2500	1.252e-03	1.9942e-05	2.000e-03	1.3941e-05	1.000e-03
0.4	0.2000	0.2006	1.121e-03	1.9536e-05	3.100e-03	1.3601e-05	2.200e-03
0.5	0.2500	0.2542	1.040e-03	1.5579e-05	1.210e-03	1.1873e-05	6.800e-03
0.6	0.4000	0.4142	9.314e-04	1.5199e-05	8.400e-03	1.0238e-05	2.200e-03
0.7	0.6500	0.6599	8.333e-04	9.1999e-04	6.000e-03	1.0017e-05	2.600e-03
0.8	1.0000	1.0016	7.456e-04	8.9387e-04	2.700e-03	9.5078e-05	0.0000
0.9	1.4500	1.4665	6.678e-04	7.8681e-04	1.720e-03	1.9536e-05	5.300e-03

Table 10. Comparison of Value of Error of Scale-2 and Scale-3 Haar Wavelets at Different Levels of Resolution.

Level of resolution	J=2	J=3	J=4
HSWM3 $L_2 error$	1.382717e-03	1.53448107e-04	1.704744e-05
HSWM3 $L_\infty error$	1.683501e-03	1.89350905e-04	2.112539e-05

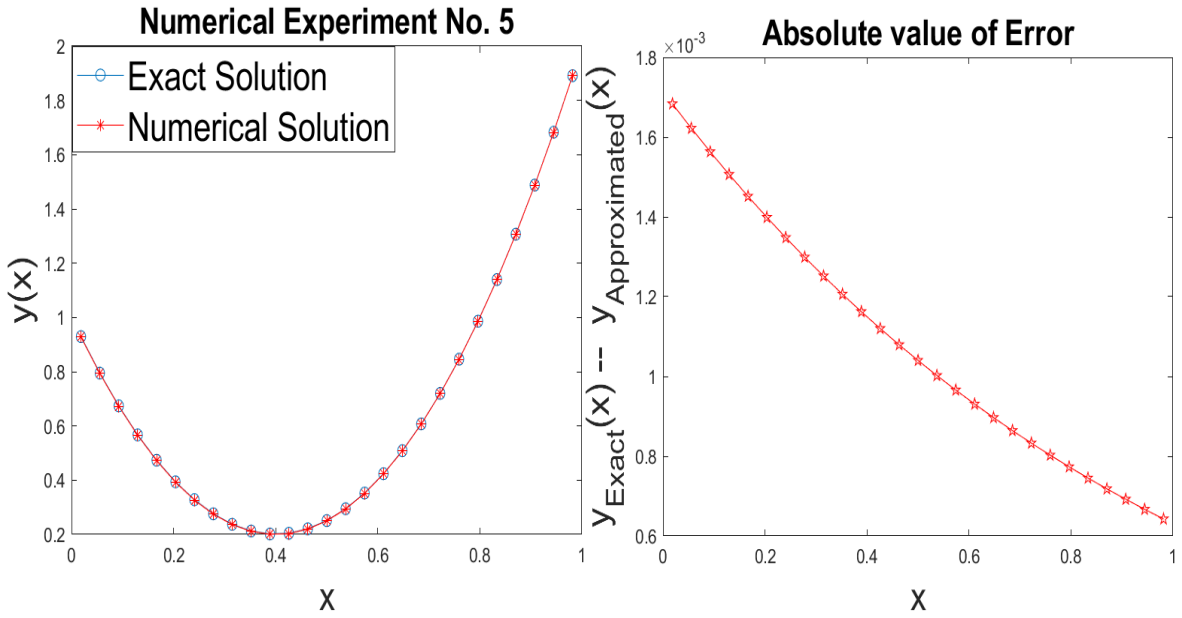

Figure 9. Graphical Representation of Exact Solutions and Numerical Solutions

DOI:https//doi.org/10.22452/mjs.vol43no1.5
Malaysian Journal of Science 43(1): 44-58 (March 2024)

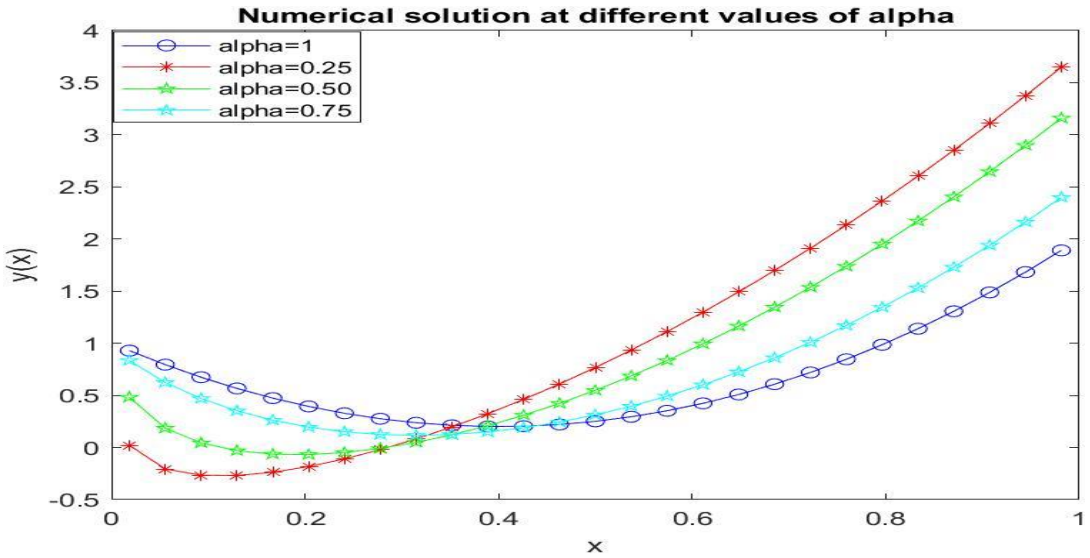

Figure 10. Graphical Representation of Numerical Solution for Different Values of α Lies Between 0 and 1. At $j = 2$ Resolution Level.

6. Conclusions and Results

The Haar scale-3 wavelet operational matrix of fractional order integration is used to solve fractional differential equations numerically in this article. This proposed method has been used to analyse both linear and non-linear problems with success. The study found that the applied technique is less complicated and more convergent than others. The proposed method is used to discuss numerical problems of this kind with reliability. Furthermore, the approaches for error analysis are thoroughly examined with the help of MATLAB, which shows good agreement of the numerical solution with the exact solution and other solutions existing in the literature. Through our study, we conclude that in the future, the proposed method could be applied to many fractional differential equations to generate more precise findings or to equations that have higher-order fractional derivatives.

7. Acknowledgement

The authors of this manuscript greatly appreciate the support provided by the Department of Mathematics, School of Chemical Engineering and Physical Sciences, Lovely Professional University, while writing this paper

8. Referencences

Almeida, R., & Bastos, N. R. O. (2016). A numerical method to solve higher-order fractional differential equations. *Mediterranean Journal of Mathematics*, *13*(3), 1339–1352.

Amin, R., Shah, K., Asif, M., Khan, I., & Ullah, F. (2021). An efficient algorithm for numerical solution of fractional integrodifferential equations via Haar wavelet. *Journal of Computational and Applied Mathematics*, *381*, 113028.

Arora, G., Kumar, R., & Kaur, H. (2020). Scale-3 Haar wavelet and Quasi-linearisation based hybrid technique for solution of coupled space-time fractional-Burgers' equation. *Pertanika Journal of Science & Technology*, *28*(2), 579–607.

Baleanu, D., & Shiri, B. (2018). Collocation methods for fractional differential equations involving non-singular kernel. *Chaos, Soliton & Fractals*, *116*, 136–145.

Chen, Y., Yi, M., & Yu, C. (2012). Error analysis for numerical solution of fractional differential equation by Haar wavelets method. *Journal of Computational Science*, *3*(5), 367–373.

Das, S. (2011). *Functional fractional calculus*. Springer.

Gowrisankar, A., & Uthayakumar, R. (2016). Fractional calculus on fractal interpolation for a sequence of data with countable iterated function system. *Mediterranean Journal of Mathematics*, *13*(6), 3887–3906.

Kobra, R., & Mohsen, R. (2021). Fractional-order Boubaker wavelets method for solving fractional Riccati differential equations. *Applied Numerical Mathematics*, *168*, 221–234.

Kumar, R., & Bakhtawar, S. (2022). An improved algorithm based on Haar scale 3 wavelets for the numerical solution of Integro-differential equations. *Mathematics in Engineering, Science & Aerospace (MESA)*, *13*(2), 617–633.

Kumar, R., & Gupta, J. (2022). Numerical analysis of linear and non-linear dispersive equation using Haar scale-3 wavelet. *Mathematics in Engineering, Science & Aerospace (MESA)*, *13*(4), 993–1006.

Li, C., & Zeng, F. (2015). *Numerical methods for fractional calculus*. Chapman & Hall/CRC.

DOI:https//doi.org/10.22452/mjs.vol43no1.5
Malaysian Journal of Science 43(1): 44-58 (March 2024)

Miller, K. S., & Ross, B. (1993). *An introduction to the fractional calculus and fractional differential equations*. Wiley.

Mittal, R. C., & Pandit, S. (2018a). New scale-3 Haar wavelets algorithm for numerical simulation of second order ordinary differential equations. *Proceedings of the National Academy of Sciences, India Section A: PhysicalSciences*, *89*(4), 799–808.

Mittal, R. C., & Pandit, S. (2018b). Quasi-linearized scale-3 Haar wavelets-based algorithm for numerical simulation of fractional dynamical systems. *Engineering Computations (Swansea, Wales)*, *35*(5), 1907–1931.

Odibat, Z., & Momani, S. (2008). Modified homotopy perturbation method: Application to quadratic Riccati differential equation of fractional order. *Chaos, Solitons & Fractals*, *36*(1), 167–174.

Oldham, K. B., & Spanier, J. (1974). *The fractional calculus: Theory and applications of differentiation and integration to arbitrary order*. Academic Press.

Podlubny, I. (1999). *Fractional differential equations*. Academic Press.

Saeed, U., & Rehman, M. U. (2013). Haar wavelet–Quasi-linearization technique for fractional nonlinear differential equations. *Applied Mathematics and Computation*, *220*, 630–648.

Shah, F. A., Abass, R., & Debnath, L. (2017). Numerical solution offractional differential equations using Haar wavelet operational matrix method. *International Journal of Applied and Computational Mathematics*, *3* (3), 2423–2445.

Shah, K., Khan, Z. A., Ali, A., Amin, R., Khan, H., and Khan, A. (2022). Haar wavelet collocation approach for the solution of fractional order COVID-19 model using Caputo derivative. *Alexandria Engineering Journal*, *59*(5), 3221–3231.

Shiralashetti, S. C., & Deshi, A. B. (2016). Haar wavelet collocation method for solving Riccati and fractional Riccati differential equations. *Bulletin of Mathematical Sciences and Applications*, *17*, 46–56.

Su, H., Chen, W., Li, C., & Chen, Y. (2012). Finite difference schemes for variable-order time fractional diffusion equation. *International Journal of Bifurcation and Chaos in Applied Sciences and Engineering*, *22*(04), 1250–1085.

DOI:https//doi.org/10.22452/mjs.vol43no1.5
Malaysian Journal of Science 43(1): 44-58 (March 2024)